Asian Journal of Conservation Biology, July 2023. Vol. 12 No. 1, pp. 100–110 AJCB: FP0215/82582
ISSN 2278-7666 ©TCRP Foundation 2023 https://doi.org/10.53562/ajcb.82582

Research Article

A new species of the genus *Hemidactylus* Goldfuss, 1820 (Squamata: Gekkonidae) from Tamil Nadu, India

Amit Sayyed[1*], Samson Kirubakaran[1, 3], Rahul Khot[2], Omkar Adhikari[2], Ayaan Sayyed[1,4], Masum Sayyed[1,4], Jayaditya Purkayastha[1,5], Shubhankar Deshpande[1,6], Shauri Sulakhe[1, 6]

[1] *Wildlife Protection and Research Society (WLPRS), Maharashtra, India*
[2] *Bombay Natural History Society, Mumbai, Maharashtra, India*
[3] *Department of Rural Development Science, Arul Anandar college, karumathur, Madurai, Tamil Nadu, India* 62551
[4] *Podar International School, Satara, Maharashtra, India*
[5] *Help Earth, 16, RNC Path, Lachitnagar, Guwahati 781007, Assam, India*
[6] *InSearch Environmental Solutions (IES), Flat No:1, Omkar apartment, Kothrud, Pune, India*

(Received: May 21, 2023 ; Revised: July 13, 2023; Accepted: July 15, 2023)

ABSTRACT

We describe a new species of *Hemidactylus* Goldfuss, 1820 based on morphological and molecular evidence from Madurai district, Tamil Nadu India. The new species shows a divergence of 8.5–30.9% on the ND2 gene from the congeners and was recovered as a member of the *Hemidactylus acanthopholis* Mirza & Sanap, 2014 sub-clade from the *Hemidactylus prashadi* Smith, 1935 clade. Further, the new species can be distinguished from other members of the *H. acanthopholis* sub-clade by having non-overlapping morphological characters and unique dorsal scalation. The distinguishing characteristics of the new species include medium body size, the number of dorsal tubercle rows at mid-body, the number of enlarged tubercles in paravertebral rows, the number of femoral pores and poreless scales separating the left and right series on the femoral-precloacal row in males, and the number of ventral scales across the belly at mid-body.

Key words: *Hemidactylus acanthopholis* sub-clade, Peninsular India, taxonomy, ND2 gene

INTRODUCTION

Members of the genus *Hemidactylus* Goldfuss, 1820 can be found across a broad range of habitats in the Old World tropics and subtropics, as well as in the Mediterranean region and America (Giri & Bauer, 2008). Certain *Hemidactylus* species have experienced both natural dispersal and human-induced introduction, leading to their establishment in previously unoccupied regions (Kluge, 1969; Vanzolini, 1978; Carranza *et al.* 2000; Vences *et al.* 2004). Globally, the genus is represented by around 188 species of which about 55 species can be found in India (Khandekar *et al.* 2023; Uetz *et al.* 2023). The Indian species of *Hemidactylus* can be classified into three major clades (Agarwal *et al.* 2019) which include *Hemidactylus flaviviridis Rüppell*, 1835; *Hemidactylus brookii* Gray, 1845 + *Hemidactylus frenatus Duméril & Bibron, 1836* and *Hemidactylus prashadi* Smith, 1935.

The *Hemidactylus prashadi* Smith, 1935 clade currently consists of 22 species distributed across peninsular India and Sri Lanka (Narayanan *et al.* 2023). Agarwal *et al.* (2019) further subdivided the *H. prashadi* clade into the northern (north of 14° N) and southern (south of 13° N) clades. The southern clade contains four sub-clades *Hemidactylus acanthopholis* Mirza & Sanap, 2014; *Hemidactylus depressus* Gray, 1842 + *Hemidactylus scabriceps* Annandale, 1906 and *Hemidactylus graniticolus* Agarwal *et al.* 2011. Amongst these, *H. acanthopholis* sub-clade consists of four nominate species *H. acanthopholis*, *Hemidactylus paaragowli* Srikanthan *et al.* 2018, *Hemidactylus vanam* Chaitanya *et al.* 2018 and *Hemidactylus sirumalaiensis* Khandekar *et al.* 2020. In this paper, we describe a new species from the *H. acanthopholis* sub-clade from Madurai, Tamil Nadu, India based on morphology and molecular comparisons.

MATERIALS AND METHODS

Sampling

Two adult males and an adult female of the new species were collected during our fieldwork in parts of Madurai, Tamil Nadu, India. All specimens were collected by hand, photographed in life, and then euthanized using halothane following the guidelines of Leary *et al.* (2013). Thigh tissue was used for further molecular work. The specimens were subsequently fixed in 4% formaldehyde for ~24 hours, washed in water and later transferred to 70% ethanol for long-term preservation. Scalation and other morphological characters were recorded using a Lensel stereo microscope. The material referred to in this study is deposited in the collection of the Bombay Natural History Society (BNHS), Mumbai, Maharashtra, India.

Morphological study

Measurements and meristic data from the collected specimens for this study were undertaken using a Yamayo digimatic calliper, a Mitutoyo 500, (to the nearest 0.1 mm). Morphological data were recorded as snout-vent length (SVL), distance from tip of snout to anterior

[*]*Corresponding Author's E-mail: amitsayyedsatara@gmail.com*

margin of vent; axilla-groin length (AG), distance from axilla to groin; trunk width (TW), maximum width of the body; eye diameter (ED), horizontal diameter of the orbit; eye-to-nares (EN), distance between anterior point of the orbit to the posterior part of the nostril; snout length (ES), distance from anterior margin of the orbit to the tip of the snout; eye-to-ear (ET), distance from posterior margin of the orbit to the anterior margin of the ear opening; internarial distance (IN), least distance between the inner margins of the nostrils; ear opening diameter (EOD), horizontal distance from the anterior to posterior margin of the ear opening; head length (HL), distance from tip of snout to posterior edge of mandible; head width (HW), maximum width of the head; head depth (HD), maximum depth of the head; inter-orbital distance (IO), shortest distance between the superciliary scale rows; upper arm length (UAL), distance from axilla to elbow, lower arm length (FAL), distance from elbow to wrist; palm length (PAL), distance from wrist to the tip of the longest finger; Finger length (FL), distance from the tip of the finger to the nearest fork; femur length (FEL), distance from groin to the knee; tibia length (TBL), distance from knee to heel toe length (TOL), distance from tip of 1st toe to the nearest fork; tail length (TL), distance between posterior margin of vent to the tip of the tail.

Meristic data recorded for all specimens included number of supralabials (SupL) and infralabials (InfL) on left (L) and right (R) sides; number of supraciliaries (SuS); number of inter-orbital scales (InO); number of scales between eye to tympanum (BeT), from posterior-most point of the orbit to anterior-most point of the tympanum; number of the postnasal (PoN),all scales posterior to the naris; number of postmentals (PoM); number of supranasal (SuN), excluding the smaller scales between the larger supranasals; number of canthal scales (CaS), number of scales from posterior-most point of naris to anteriormost point of the orbit; number of enlarged dorsal paravertebral tubercles (PvS), between pelvic and pectoral limb insertion points; number of mid-dorsal enlarged tubercles (MbS), from the centre of mid-dorsal row diagonally towards the ventral scales; number of mid-ventral scales (MvS), from the first scale posterior to the mental to last scale anterior to the vent; number of mid-body scales (BlS), across the ventral between the lowest rows of dorsal scales at mid-body; femoral pores (FPores), the number of femoral pores; poreless scales (PS), number of poreless scales between left and right femoral pores and the number of undivided lamellae on the right digits in manus (MLamR) and pes (PLamR). Morphometric data are given as % of SVL. For the geographical coordinates and altitude we used a Kestrel 4500 receiver.

Molecular analysis

DNA extraction, amplification, and sequencing: DNA extraction, amplification and sequencing protocols for ND2 as per (Sayyed *et al.* 2023) were followed. The genomic DNA of *Hemidactylus* specimen (male; BNHS 2919) was extracted from thigh muscle tissue that was preserved in 100% ethanol. DNA extraction was carried out using a DNeasy (QiagenTM) blood and tissue kit following the manufacturer's instructions. Partial sequences of the mitochondrial NADH dehydrogenase 2 ND2) gene for new species were amplified. The amplification of the ND2 gene was carried out in three steps of polymerase chain reaction (PCR) using primers MetF1 (forward) and H5934 (reverse) (Macey *et al.* 1997). The fragments were amplified with the following conditions: 95°C – 3 min, 1 cycle, 95°C – 30 sec, 56–58°C – 30 sec, 72°C – 45 sec, 35 Cycles, 72°C – 7 min. Forward and reverse DNA strands were sequenced using a BDT v3.1 Cycle sequencing kit on ABI 3730xl Genetic Analyzer.

Sequence alignments: The ND2 sequences generated in the study (Table 1) were cleaned manually in MEGA v.7 (Kumar *et al.* 2016) using chromatograms visualised in Chromas v.2.6.5 (Technelysium Pty. Ltd.). Comparative ND2 sequences comprising members of *Hemidactylus* were downloaded from GenBank® (Benson *et al.* 2017) following (Narayanan *et al.* 2023) and newly generated sequences were deposited in the GenBank® under accession numbers as per Table 1. The sequences were aligned using MUSCLE (Edgar, 2004) implemented in MEGA v.7 (Tamura & Nei, 1993, Kumar *et al.* 2016) with default parameter settings. The final ND2 alignment contained 36 sequences (35 ingroups and 1 outgroup) with 1044 base pair (bp) lengths. This ND2 alignment was used for phylogenetic analyses. *Dravidogecko douglasadamsi* Chaitanya *et al.* 2019 (MN520270) was used as an outgroup to root the phylogenetic analyses.

Molecular phylogenetics analysis: Maximum Likelihood (ML) and Bayesian Inference (BI) methods of phylogenetic analyses were implemented. The ND2 region was partitioned per codon position. Model search for the ML analysis was performed with a greedy search algorithm (Schwarz, 1978) and models were selected using the Akaike Information Criterion (AIC). Maximum Likelihood analysis was performed using the web implementation of IQ-tree (Nguyen *et al.* 2015) under the following models of sequence evolution: TVM+F+I+G4 for position 1, TPM3+F+G4 for position 2, TN+F+I+G4 for position 3. The models of sequence evolution were determined using ModelFinder (Kalyaanamoorthy *et al.* 2017) on the IQ-tree web platform, and branch support was tested using 1000 non-parametric rapid ultrafast bootstrap pseudo-replicates (Minh *et al.* 2020). Bayesian trees were generated using MrBayes v.3.2.6 (Ronquist *et al.* 2012). Model search for the BI analysis was performed with a greedy search algorithm (Schwarz, 1978) and models were selected using the Bayesian Information criterion (BIC). The best substitution model for BI phylogenetic analysis was determined using PartitionFinder v.1.1.1 (Lanfear *et al.* 2012). The models of sequence evolution were as follows: GTR+I+G for codon positions 1 and 3, HKY+G for codon position 2. For the BI analysis, two simultaneous, independent analyses were run starting from different random trees. Three heated and one cold chains were used in the analysis. The analysis was run for 10 million generations and Markov chains were sampled every 200 generations. At the end of the run, we tested the convergence by checking the standard deviation of split frequencies, which was less than 0.001, and by checking the trace plots using Tracer v.1.7 (Rambaut *et al.* 2018). The Effective Sample Size (ESS) values for all the parameters were above 200, further indicating convergence. A total of 25% of trees were discarded as burn-in. The tree representing the best evolutionary hypothesis was selected using a 50% majority consensus rule.

Genetic divergence (*p*-distance): The *p*-distances were calculated for the ND2 gene in MEGA v.7. The

variance estimation method was kept as none. The substitution type was set as nucleotide, the model was kept as *p*-distance and the substitutions were included as d: transition + transversions. The pattern among lineages was ket as Same (Homogeneous). The resultant *p*-distances are mentioned in Table 2.

Table 1. List of GenBank® accession numbers of ND2 sequences used for the phylogenetic analyses in this study. The Genbank accession number with an asterisk (*) indicates the sequence generated in this study.

Sr no	Species	Genbank Accession No.	Voucher	Locality
1	*H. aaronbaueri*	MZ682617	NRC-AA-1138	India, Maharashtra, Pune, Malshej Ghat
2	*H. acanthopholis*	MG711530	CES 14009	India, Tamil Nadu, Tirunelveli, Kallidaikurichi
3	*H. acanthopholis*	MG711531	CES 17066	India, Tamil Nadu, Tirunelveli, Kallidaikurichi
4	*H. depressus*	HM559621	ADS 29A	Sri Lanka, Galkotte
5	*H. depressus*	HM559625	AMB 7481	Sri Lanka, Matale
6	*H. easai*	OM487119	BNHS 3103	India, Kerala, Palakkad dist, Attapadi
7	*H. easai*	OM487118	ZSI/WGRC/ IR.V/3471	India, Kerala, Palakkad dist, Attapadi
8	*H. graniticolus*	MK569812	AK 348	India, Karnataka, Bangalore Rural, Harohalli
9	*H. hunae*	HM559640	AMB 7416	Sri Lanka, Pitakumbura
10	*H. kangerensis*	MK569822	CES 14190	India, Andhra Pradesh, East Godavari, VR Puram
11	*H. kangerensis*	MK569824	BNHS 2486	India, Chhattisgarh, Bastar, Kanger Valley National Park
12	*H. kolliensis*	MK569825	BNHS 2537	India, Tamil Nadu, Dharmapuri, Kollimalai Ghat
13	*H. kolliensis*	MT943048	NCBS BH736	India, Tamil Nadu, Perambalur, Pachaimalai
14	*H. maculatus*	MK569827	AK 062	India, Maharashtra, Pune, Mulshi
15	*H. maculatus*	MK569830	AK 065	India, Maharashtra, Raigad, Matheran
16	***H. multisulcatus sp. nov.***	OR360374*	BNHS 2919	India, Tamil Nadu, Madurai District, SVN college, near Nagamalai
17	*H. paaragowli*	MK802893	CESL 274	India, Kerala, Kollam District, Devarmalai-Sivagiri Hill Complex
18	*H. paaragowli*	MN496393	CESL 273	India, Kerala, Kollam District, Devarmalai-Sivagiri Hill Complex
19	*H. pakkamalaiensis*	OQ957153	BNHS 2911	India, Tamil Nadu, Villupuram district, Pakkamalai hill
20	*H. pakkamalaiensis*	OQ957154	BNHS 2907	India, Tamil Nadu, Villupuram district, Pakkamalai hill
21	*H. paucifasciatus*	MK569847	ZSI-R-28357/ CES 15248	India, Odisha, Keonjhar, Anandapur, Gadachandi Temple
22	*H. paucifasciatus*	OQ595083	ZSI-R-28526	India, Odisha, Keonjhar, Anandapur, Chakratirtha
23	*H. prashadi*	MK569843	CESG 359	India, Maharashtra, Kolhapur, Patgaon
24	*H. sahgali*	MG742362	NCBS-AU709	India, Maharashtra, Pune, Saswad
25	*H. scabriceps*	MH454769	CES 12008	India, Tamil Nadu, Tirunelveli, Tirunelveli
26	*H. sirumalaiensis*	MT943051	NCBS-BH744/ AK 909	India, Tamil Nadu, Dindigul, Sirumalai
27	*H. sirumalaiensis*	MT943050	NCBS-BH743/ AK 908	India, Tamil Nadu, Dindigul, Sirumalai
28	*H. siva*	MK569845	NHM.OU.REP.H	India, Karnataka, Bellary, Hampi
29	*H. sushilduttai*	MK569852	CES 11079/ NCBS-AU 157	India, Andhra Pradesh, Visakhapatanam, Simhachalam
30	*H.tamhiniensis*	MN482222	CES 14023	India, Maharashtra, Pune, Tamhini Ghat
31	*H. triedrus*	MH666065	NCBS-AU703	India, Andhra Pradesh, Nellore, Nellore
32	*H. vanam*	MK569853	CESG 392	India, Tamil Nadu, Madurai, Saptur
33	*H. vanam*	MK569854	CESG 393	India, Tamil Nadu, Madurai, Saptur
34	*H. vanam*	MK569855	CESG 394	India, Tamil Nadu, Madurai, Saptur
35	*H. whitakeri*	MH666066	NCBS-AU713	India, Kodalagurki village, Bangalore rural District
36	*Dravidogecko douglasadamsi*	MN520270	BNHS 2349	India, Tamil Nadu state, Tirunelveli district, Manjolai estate

Taxonomy

Family: Gekkonidae Gray, 1825

Genus: *Hemidactylus* Goldfuss, 1820

***Hemidactylus multisulcatus* sp. nov.,** Figs 1, 2, 3, 4

http://zoobank.org/urn:lsid:zoobank.org:act:04F27A02-6E00-428D-A306-6359DDAB4718

Holotype. An adult male, BNHS 2918, collected from one meter above ground on the wall of SVN college, near Nagamalai, (9° 56' 12.6168" N 78° 2' 38.8752" E; ca. 168.6 m asl.), Madurai District, Tamil Nadu, India; by Amit Sayyed and Samson Kirubakaran on 27 January 2023.

Paratype. An adult male, BNHS 2919 and an adult female, BNHS 2920; collection details same as the holotype.

Diagnosis. A medium-sized gecko of the genus *Hemidactylus*, snout to vent length less than 84 mm (n = 3); 11 supralabials; 9–10 infralabials; dorsal pholidosis heterogenous, composed of small, granular, round, smooth scales intermixed with enlarged, much regularly arranged, strongly keeled, slightly pointed enlarged tubercles, two rows of enlarged tubercles on the paravertebral region smaller than those on mid-body enlarged shell or bivalve-like tubercles, few slightly small on lower flanks; shell or bivalve-like enlarged tubercles adorned with multiple grooves; 25–27 paravertebral tubercles between forelimb and hind limb insertions; mid-dorsal enlarged tubercles 17–19; scales on the snout, canthus rostralis, forehead and inter-orbital re-gion round, juxtaposed; periocular scales weakly keeled, much larger than those on snout; single elongated, enlarged supranasal on each side, separated from each other by two vertically arranged, small, round scales; scales on ventral surface of neck, chest, arm, pes and tail smooth, cycloid, mid-ventral scales 161–177, mid-body scales 35–36 across the belly between the lowest rows of dorsal scales; ten or eleven lamellae under digit IV of manus and pes; males with continuous series of 18–20 femoral pores (n = 2), six or seven poreless scales between femoral pores; dorsal scales of thigh and tibia small, granular, smooth, intermixed with regularly arranged, keeled enlarged tubercle; postcloacal spur absent on each side; dorsal scales at tail base and on tail small, granular scales similar in size and shape to those on mid-body dorsum, gradually becoming larger, intermixed with series of 4–6 much enlarged, pointed, keeled, conical tubercles forming whorls; ventral scales at tail base subequal, smooth, imbricate, fairly larger than mid-body ventral scales; ventral scales with a median row of large, undivided, rectangular, plate-like subcaudal scales covering almost entire portion of the tail; median row bordered laterally by one or two rows of large, smooth, imbricate triangular scales, four brown circular faint blotches on dorsal body between neck and hind limb insertion.

Comparison with members of the *H. prashadi* clade.

Hemidactylus multisulcatus **sp. nov.** can be easily distinguished from the other congeners of the group based on several non-overlapping morphological characters. The new species is a member of the *H. prashadi* group and can be easily distinguished from all twenty-two members of the group by a combination of the following differing or non-overlapping characters: SVL less than 84 mm (vs. more than 100 mm in *H. aaronbaueri* Giri, 2008, *H. easai* Das *et al.* 2022, *H. graniticolus* Agarwal *et al.* 2011, *H. hegdei* Pal & Mirza 2022, *H. hunae* Deraniyagala, 1937, *H. kimbulae* Amarasinghe *et al.* 2021, *H. maculatus* Dumeril & Bibron, 1836, *H. paaragowli* Srikanthan *et al.* 2018, *H. paucifasciatus* Mohapatra *et al.* 2023, *H. pakkamalaiensis* Narayanan *et al.* 2023, *H. siva* Srinivasulu *et al.* 2018, *H. sushilduttai* Giri *et al.* 2017, *H. tamhiniensis* Khandekar *et al.* 2021, *H. vanam* Chaitanya *et al*. 2018 and less than 65 mm in *H. gujaratensis* Giri *et al.* 2009, *H. triedrus* Daudin, 1802, *H. scabriceps* Annandale, 1906, *H. whitakeri* Mirza *et al.* 2018); dorsal pholidosis heterogenous, composed of small, granular scales intermixed much regularly arranged, strongly keeled, enlarged tubercles (vs. irregularly arranged, enlarged, feebly keeled dorsal tubercles in *H. aaronbaueri* Giri, 2008, *H. gujaratensis*, *H. hunae*, *H. kimbulae*, *H. siva* and homogenous dorsal pholidosis of imbricate scales, lacking enlarged tubercles in *H. scabriceps*); 25–27 paravertebral tubercles (vs. 18–20 in *H. aaronbaueri, H. acanthopholis, H. easai*, *H. graniticolus*, *H. hegdei*, *H. kangerensis* Mirza *et al.* 2017, *H. kolliensis* Agarwal *et al.* 2019, *H. maculatus,* 21–24 in *H. paaragowli*, *H. paucifasciatus*, 53–58 in *H. pieresii* Kelaart 1852, 34–38 in *H. pakkamalaiensis*, 22–26 in *H. sirumalaiensis*, 29–32 in *H. tamhiniensis*, less than 17 in *H. depressus*, *H. gujaratensis*, *H. hunae*, *H. kimbulae*, *H. sahgali* Mirza *et al.* 2018, *H. siva*, *H. sushilduttai*, *H. whitakeri* Mirza *et al.* 2018); regularly arranged, keeled enlarged tubercle on the dorsal region of thigh and tibia (vs. absent in *H. aaronbaueri*, *H. depressus*, *H. graniticolus*, *H. gujaratensis*, *H. hegdei*, *H. hunae*, *H. kimbulae*, *H. paaragowli*, *H. pieresii*, *H. prashadi* Smith, 1935, *H. scabriceps*, *H. tamhiniensis*); males with continuous series of 18–20 Fpores and six or seven PS (vs. 13–14 PS in *H. acanthopholis*, 15–19 Fpores and 2–4 PS in *H. depressus*, 24–30 Fpores and 2–4 PS in *H. easai*, 23–28 Fpores and 1–3 PS in *H. graniticolus* and *H. gujaratensis*,14–15 Fpores and 11 PS in *H. hegdei*, 22–24 Fpores and 3–6 PS in *H. hunae*, 21–24 Fpores in *H. kimbulae*, 21–25 Fpores and two or three PS in *H. kolliensis*, 16–19 Fpores and 5–9 PS in *H. maculatus*, 10–12 Fpores and 16–18 PS in *H. paaragowli*, 12–13 Fpores and three or four PS in *H. paucifasciatus*, 17–20 Fpores and 1–3 PS in *H. pieresii*, 17–20 Fpores and three PS in *H. prashadi*, 11–15 Fpores and 1–3 PS in *H. sahgali*, 16–18 Fpores and 13–15 PS in *H. sirumalaiensis*, 17 or 18 Fpores and five PS in *H. siva*, 20–23 Fpores and 3–6 PS in *H. sushilduttai*, 17–18 Fpores in *H. tamhiniensis*, 7–9 Fpores and 1–3 PS in *H. triedrus*, 17–22 Fpores and ten or 11 PS in *H. vanam*, seven or eight Fpores and three PS in *H. whitakeri* and only precloacal pores present in *H. scabriceps*); mid-body scales 35–36 (vs. more than 40 in *H. aaronbaueri*, *H. easai*, *H. graniticolus*, *H. tamhiniensis* and less than 35 in *H. depressus*, *H. hegdei*, *H. kolliensis*, *H. maculatus*, *H. paaragowli*, *H. paucifasciatus*, *H. pieresii*); postcloacal spur absent on each side (vs. present in *H. aaronbaueri*, *H. acanthopholis*, *H. depressus*, *H. paaragowli*, *H. pakkamalaiensis*, *H. paucifasciatus*, *H. sahgali*, *H. scabriceps*, *H. sushilduttai*, *H. triedrus, H. whitakeri*); four brown circular faint blotches on dorsal body between neck to hind limb insertion (vs. three to five transverse bands in *H. aaronbaueri*, *H. acanthopholis*, *H. kangerensis*, *H. paucifasciatus*, *H. sahgali*, *H. sushilduttai*, *H. triedrus*, *H. whitakeri*, "I" shaped markings in *H. paaragowli*, four or five dark markings in *H. depressus*, *H. hegdei*, *H. maculates*, *H. sirumalaiensis*, *H. siva*, *H. tamhiniensis*, dark spots in transversely arranged rows in *H. gujaratensis*, *H. prashadi*, *H. scabriceps*, a vertical line at

dorso-lateral region each side in *H. pieresii*, five to five transverse saddle like bands in *H. easai*, *H. graniticolus*, *H. hunae*, *H. kimbulae*, *H. kolliensis*, *H. pakkamalaiensis* and *H. vanam*. Additionally, within *prashadi* group, the new species stands out with its exceptional characteristics: it possesses a highly distinctive shell or bivalve-like enlarged tubercles adorned with multiple grooves, setting it apart from all other known species.

Description of the holotype. Adult male, in good state of preservation. SVL 72.77 mm, head short (HL/SVL 0.28), slightly wide (HW/HL 0.69), not depressed (HD/HL 0.42), distinctly larger from neck. Loreal region slightly inflated, canthus rostralis in-distinct. Snout short (ES/HL 0.39); scales on the snout, canthus rostralis, forehead and inter-orbital re-gion heterogeneous, scales on snout and canthus rostralis large, round, juxtaposed, larger than those on forehead and inter-orbital region, periocular scales weakly keeled, much larger than those on snout; head dorsum, temporal and occipital region with much smaller scales intermixed with randomly arranged, weakly keeled, conical, enlarged tubercles; enlarged tubercles on head dorsum, temporal and occipital region smaller than those on nape and shoulder (Fig. 2 A). Eye small (ED/HL 0.23), pu-pil vertical with crenulated margins; supraciliaries not elongate, small, mucronate, gradually increasing in size towards the front of the orbit; ear-opening oval in shape, very small (EOD/HL 0.10); eye to ear distance much longer then diameter of eye (ET/EOD 2.81). Rostral much wider (2.40 mm) than high (1.45 mm), divided by a weakly developed rostral groove; single, elongated, enlarged supranasal on each side, separated from each other by two vertically arranged, small, round scales; rostral in contact with supralabial I, nasal, supranasal and internasal; nostrils very small, oval, bordered by postnasals, supranasal and rostral; two rows of small scales separate the orbit from the supralabials (Fig. 2 C). Mental enlarged, subtriangular, pointed posteriorly, wider (2.37 mm) than long (2.56 mm); two pairs of postmentals, inner pair much larger than outer pair; scales on throat and gular region small, granular, juxtaposed, smooth (Fig. 2 B). Supralabials up to angle of jaw eleven on each side; supralabial I slightly smaller than II; infralabials up to angle of jaw nine on the right and ten on the left side; infralabial I smaller than II in size. Canthal region with 21 scales on both sides; supraciliaries separated by 50 scales at midorbit. Body relatively short, trunk less than half of SVL (AG/SVL 0.41), ventrolateral folds visibly distinct. Dorsal pholidosis heterogeneous; small, granular, round, smooth scales intermixed with enlarged, much regularly arranged, strongly keeled, slightly pointed shell or bivalve-like multi-grooved enlarged tubercles, two rows of enlarged tubercles on the paravertebral region smaller than those on mid-body enlarged tubercles, few slightly small on lower flanks (Fig. 3 A, C); shell or bivalve-like enlarged tubercles adorned with multiple grooves (Fig. 4 A); 25 dorsal paravertebral tubercles between pectoral and pelvic limb insertion points; 18 longitudinal rows of enlarged tubercles at mid-dorsal. Small, granular scales on nape intermixed with weakly keeled enlarged tubercles, enlarged tubercles on nape and shoulder slightly smaller than those on dorsum. Scales on ventral surface of neck, chest, manus, pes and tail smooth, cycloid; ventral scales at mid-body much larger than granular scales on dorsum, mid-ventral scales 177, mid-body scales 36 across the belly between the lowest rows of dorsal scales (Fig. 3 B); 18 femoral pores on right side of thigh and 18 femoral pores on left side of thigh, seven poreless scales between femoral pores. (Fig. 2 D); Forelimbs relatively short, slender; dorsal scales of brachium smooth, flattened and subimbricate; scales of forearm smooth, flattened and subimbricate, smaller than those on brachials; ventral scales of brachium smooth, rounded, juxtaposed, smaller than those on forearm; scales beneath forearm, smooth, flattened, imbricate; palmar scales smooth, slightly raised, sub circular, juxtaposed; claws strongly curved; dorsal scales of thigh and tibia small, granular, smooth intermixed with enlarged, regularly arranged, keeled enlarged tubercle (Fig. 4 B); ventral scales of thigh and tibia flat, cycloid; plantar scales smooth, subimbricate; Fore and hind limbs relatively short, forearm short (FAL/SVL 0.19); tibia short (TBL/SVL 0.20); digits moderately short, strongly clawed; all digits of manus and digits I to IV of pes indis-tinctly webbed at base; terminal phalanx of all digits curved, arising angularly from distal portion of expanded lamellar pad, half or more than half as long as associated lamellar pad; scansors beneath each digit in a straight transverse series, divided except for distal and four to five basal scansors on digit I: 9–10–10–10–10 (right manus), 8–10–10–10–10 (right pes, Fig. 2 E, F). The relative length of digits, fingers: IV (5.38 mm)>III (5.21 mm) > V (4.93 mm)>II (4.52 mm) >I (3.24 mm); toes: IV (5.76 mm) > II (5.58 mm) >V (5.36 mm) >III (5.33 mm) > I (3.24 mm). Tail entire and original, depressed, flat beneath, verticillate, with median furrow; longer than snout-vent length (TL/SVL 1.24). Dorsal scales at tail base and on tail heterogeneous, small, granular scales similar in size and shape to those on mid-body dorsum, gradually becoming larger, intermixed with series of 4–6 much enlarged, keeled, pointed, conical tubercles forming whorls. Ventral scales at tail base subequal, smooth, imbricate, fairly larger than mid-body ventral scales; ventral scales with large, undivided, rectangular, plate-like subcaudal scales (median row) covering almost entire portion of the tail; median row bordered laterally by one or two rows of large, smooth, imbricate triangular scales (Fig. 4 D); postcloacal spur absent on each side (Fig. 4 C).

Colouration in life and preservative (Fig. 5 A, B). The dorsal aspect of the body is grey, intermixed with yellowish-brown scales on dorsal body; four brown circular blotches on dorsal body between neck and hind limb insertion. Head overall grey with brown unpatented markings dark on occipital, snout and supraciliaries dull-yellow. Dorsal aspect of the tail with nine or ten alternating brown bands. The limbs are grey above with irregular dull-brown markings; fingers are grey, black on tip. The ventral side of the head, body and limbs whitish, ventral side of tail is grey with yellowish makings. In preservative, the overall colouration is the same as in life except in brown markings on the dorsum that became dark grey.

Variation. Mensural and meristic data for the type series is given in Table 3. There are two male and a female specimens ranging in SVL from 71.80 mm to 84.00 mm. All paratypes resemble the holotype except as follows: the number of lamellae on digit I of the manus ranges from 8–9; on digit IV of the manus from 10–11; on digit I of the pes from 8–9; on digit IV of the pes from 10–11; Ventral scale counts in longitudinal and transverse series vary from 161–177 and 35–36, respectively; holotype males BNHS 2918 has 18 femoral pores on each thigh; paratype male BNHS 2919 with 19

on right thigh and 20 on left thigh. The two males and a female in the collection match each other in overall colouration.

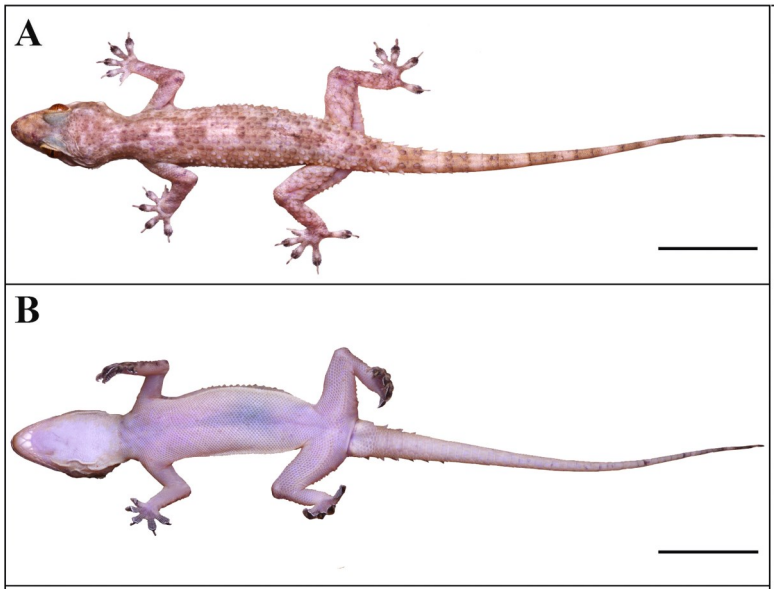

Figure 1. *Hemidactylus multisulcatus* **sp. nov.,** holotype in life, BNHS 2918; (A) dorsal view of body, (B) ventral view of body. Scale bars 10 mm.

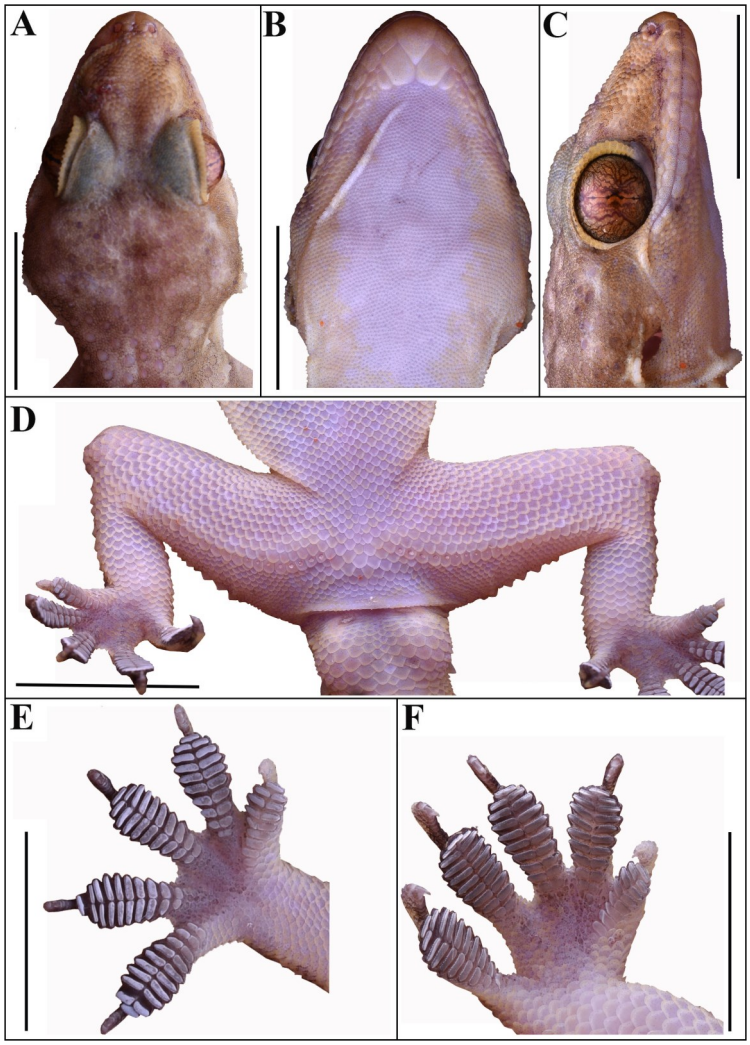

Figure 2. *Hemidactylus multisulcatus* **sp. nov.,** holotype in life, BNHS 2918; (A) dorsal view of mid-body, (B) ventral view of mid-body, and (C) lateral view of the mid-body. Scale bars 5 mm.

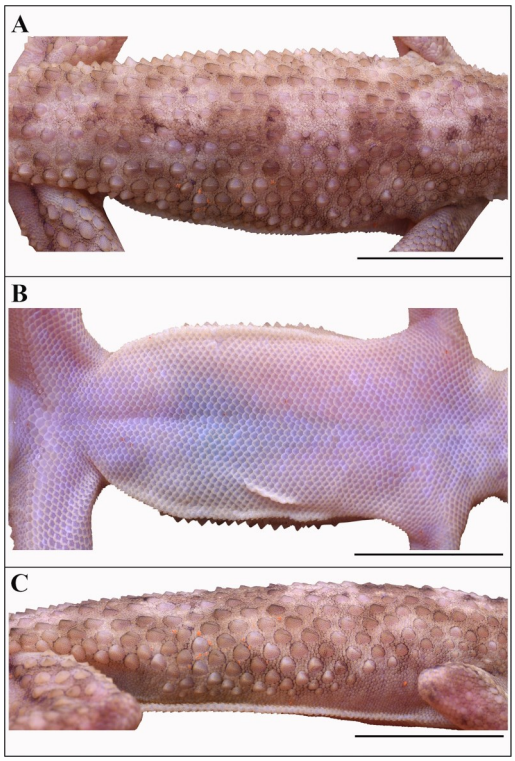

Figure 3. *Hemidactylus multisulcatus* **sp. nov.,** holotype in life, BNHS 2918; (A) dorsal view of head, (B) ventral view of head, (C) lateral view of head, (D) view of femoral and precloacal region, (E) ventral view of lamellae under right menus, and (F) ventral view of lamellae under right pes. Scale bars 5 mm.

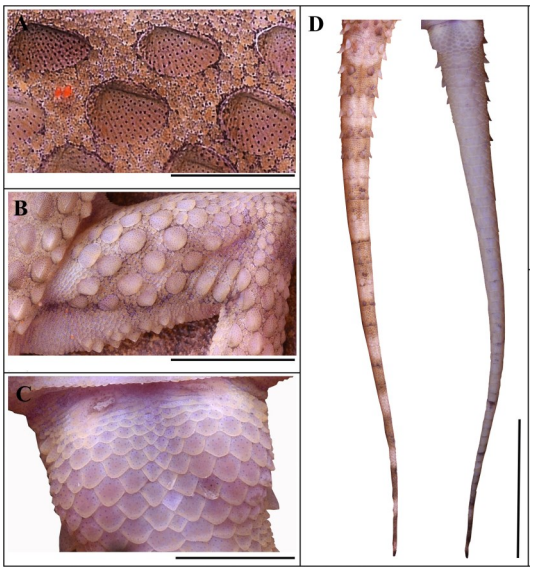

Figure 4. *Hemidactylus multisulcatus* **sp. nov.,** holotype in life, BNHS 2918; (A) showing shell-like enlarged dorsal tubercles with multiple grooves, (B) enlarged tubercle on thigh, (C) postcloacal region, (D) dorsal and ventral view of tail.

Etymology. The specific epithet indicates the unique shell or bivalve-like enlarged tubercles adorned with multiple grooves. In Latin (sulcus = groove) and English, multiple grooves = multisulcatus.

Suggested Common Name: Madurai Rock Gecko

Natural History (Fig. 5, 7).

The new species was found on the stone walls of SVN College near Nagamalai hill range, Madhurai District, Tamil Nadu, India. The individuals of the new species were also observed on the ground at night in search of prey. The type-locality is surrounded by the Nagamalai hill range which is situated about 10 km west of Madurai City. Nagamalai hill range is covered with thorny shrubs and trees. The type series was collected at night (21.00–22.00 hr). The new species was found to be sympatric with *Echis carinatus* Schneider, 1801; *Daboia russelii* Shaw & Nodder, 1797; *Ahaetulla oxyrhyncha* Bell, 1825; *Lycodon aulicus* Linnaeus, 1758 and *Ptyas mucosa* Linnaeus, 1758.

Distribution. Currently, *H. multisulcatus* **sp. nov.** is only known from its type locality SVN college, near Nagamalai hill range, (9° 56' 12.6168" N 78° 2' 38.8752" E; ca. 168.6 m asl.), in the Madurai District of Tamil Nadu State. Further research is required to clarify the extent of the distribution, population trends and conservation status of the new species.

Molecular Analysis (Fig. 6)

Phylogenetic relationships. The tree topology recovered is in agreement with the trees generated by (Narayanan *et al.* 2023). The (ML) and BI analyses based on the ND2 gene show *H. multisulcatus* **sp. nov.** to be a member of the *H. acanthopholis* sub-clade (Agarwal *et al.* 2019). *H. multisulcatus* **sp. nov.** was recovered as a sister to *H. vanam* in both ML and BI analyses with a high bootstrap (bp) support value of 99 and posterior probability (pp) value of 1. Based on the uncorrected p-distance (Table 2), the following genetic distances were recorded between the new species and the other members of *H. acanthopholis* sub-clade: 8.5–9.7% with *H. sirumalaiensis;* 8.9–9.8% with *H. vanam;* 14.8–14.9% with *H. paaragowli* and 15.3% with *H. acanthopholis.*

Figure 5. Habitat of *Hemidactylus multisulcatus* **sp. nov.,** Nagamalai, Madurai, Tamil Nadu of India.

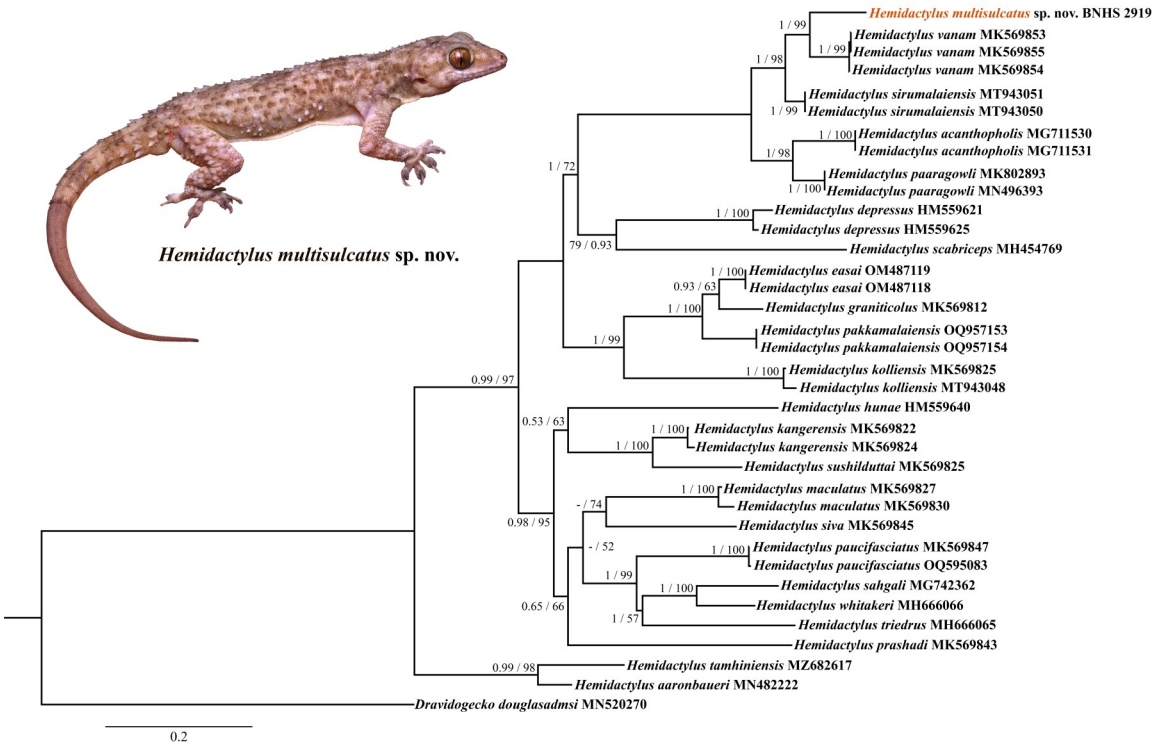

Figure 6. ML phylogeny showing the phylogenetic relationships of the *Hemidactylus prashadi* Smith, 1935 clade. Numbers at internal branches are Bayesian posterior probabilities (left) and ML bootstrap support values (right)..

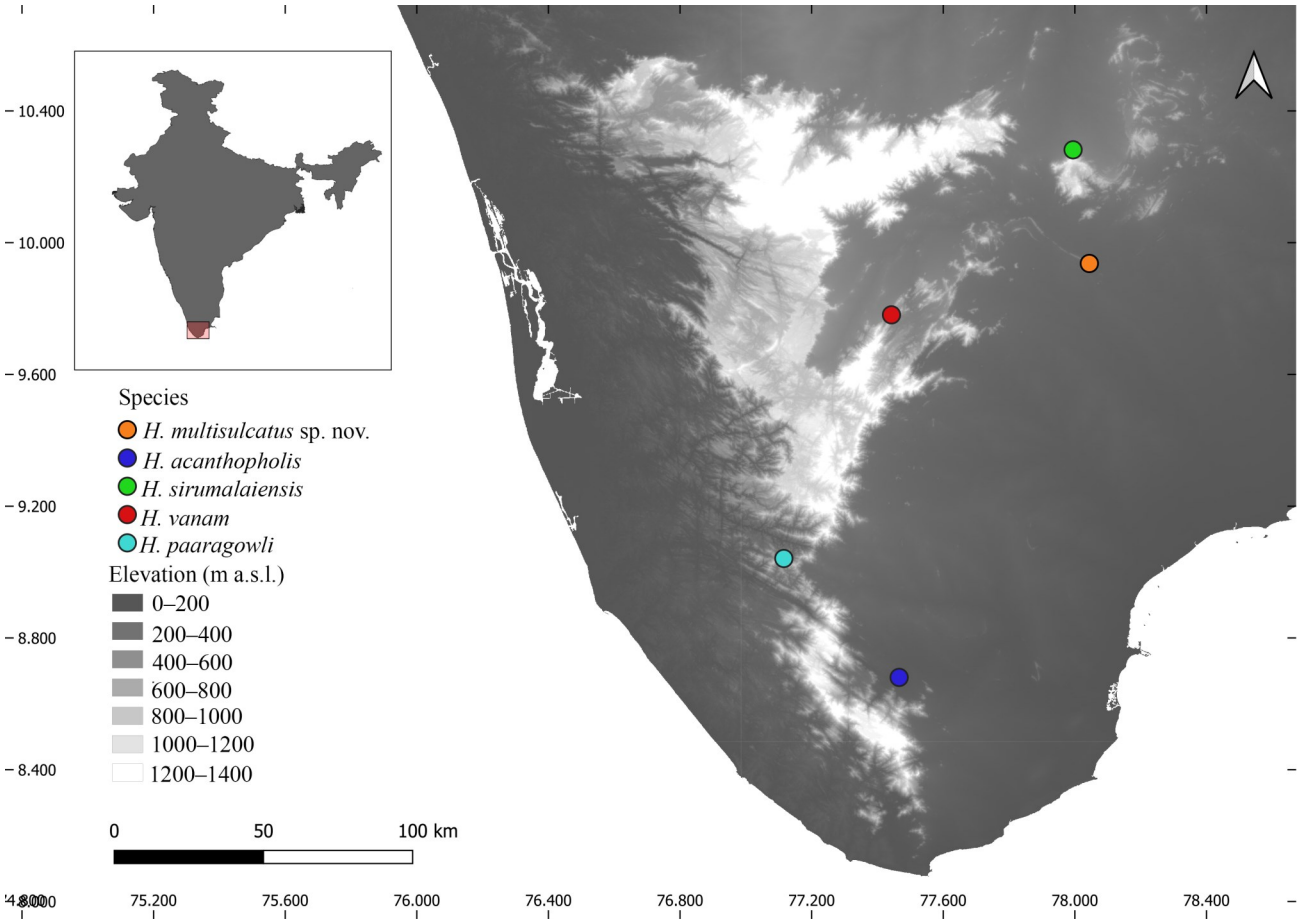

Figure 7. Map showing the distribution of the members of the *Hemidactylus acanthopholis* Mirza & Sanap, 2014 sub-clade. The circles indicate the type-localities of the species.

DISCUSSION

The *H. prashadi* clade is the most diverse clade currently represented by 22 species and has a distribution range across peninsular India and Sri Lanka (Agarwal *et al*. 2019; Khandekar *et al*. 2021; Das *et al*. 2022; Narayanan *et al*. 2023; Pal & Mirza, 2022). This addition of the new species underscores the rich biodiversity of *Hemidactylus* and highlights the importance of continued taxonomic research. The presence of shell or bivalve-like enlarged tubercles adorned with multiple grooves in *H. multisulcatus* **sp. nov.** (Fig. 4 A) is very much typical to the species which was not erstwhile observed in any of the members of the *H. prashadi* clade. The presence of distinct and unusual scales on the dorsal body of this new species may offer intriguing insights into its adaptation and ecological niche. It is believed that the reptilian scales evolved in the Mesozoic period serving different functions (Choung *et al.* 2002). Thus, understanding the genetic mechanisms underlying the formation of these scales can provide valuable insights into the evolutionary processes that shape the morphology and adaptive traits within the genus.

The discovery of *H. multisulcatus* **sp. nov.** highlights the high species diversity of the *H. prashadi* clade in southern India. This description raises the total number of species in the *H. acanthopholis* sub-clade to five. We speculate the presence of more such hitherto unknown species of *Hemidactylus* in South India that need to be discovered with dedicated sampling efforts.

The authors are thankful to the Forest Departments of Tamil Nadu for their support during field surveys. We are thankful to the Director, of Bombay Natural History Society, Mumbai for providing access to specimens and registration of the type specimens. We thank Shiva Harshan and Kamesh Salinkhe for helping us in the fieldwork. The authors are thankful to Wildlife Protection and Research Society (WLPRS) and Insearch Environmental Solutions (IES) for the laboratory facilities and institutional support. We thank anonymous reviewers for helpful comments which allowed us to improve the previous version of the manuscript.

REFERENCES

Agarwal, I., Bauer, A.M., Giri, V.B. and Khandekar, A. 2019. An expanded ND2 phylogeny of the *brookii* and *prashadi* groups with the description of three new Indian *Hemidactylus* Oken (Squamata: Gekkonidae). Zootaxa 4619 (3): 431–458. https://doi.org/10.11646/zootaxa.4619.3.2

Autumn, K., Liang, Y. A., Hsieh, S. T., Zesch, W., Chan, W. P., Kenny, T. W. and Full, R. J. 2002. Adhesive force of a single gecko foothair. Nature 405 (6787): 681-685.

Bauer, A. M. 1990. Osteological evidence for the validity of *Hemidactylus turcicus* (Sauria: Gekkonidae). Journal of Herpetology 24(4): 404-408.

Table 2. Uncorrected pairwise genetic distances between *Hemidactylus multisulcatus* **sp. nov.,** and other species in *prashadi* group.

No.	Species	1	2	3	4	5	6	7	8	9	10	11	12	13	14	15	16	17	18	19	20	21	22	23	24	25	26	27	28	29	30	31	32	33	34	35	36
1	*D. douglasadamsi (MN520270)*																																				
2	*H. multisulcatus sp. nov. (OR360374)*	0.318																																			
3	*H. aaronbaueri (MZ682617)*	0.305	0.277																																		
4	*H. acanthopholis (MG711530)*	0.336	0.153	0.272																																	
5	*H. acanthopholis (MG711531)*	0.328	0.153	0.258	0.001																																
6	*H. depressusi (HM559621)*	0.33	0.258	0.253	0.226	0.227																															
7	*H. depressus (HM559625)*	0.322	0.266	0.241	0.226	0.224	0.029																														
8	*H. easai (OM487119)*	0.331	0.258	0.236	0.24	0.228	0.209	0.201																													
9	*H. easai (OM487118)*	0.331	0.257	0.236	0.24	0.229	0.209	0.2	0																												
10	*H. graniticolus (MK569812)*	0.336	0.269	0.233	0.238	0.227	0.216	0.205	0.07	0.07																											
11	*H. hunae (HM559640)*	0.325	0.281	0.287	0.26	0.261	0.235	0.232	0.229	0.228	0.237																										
12	*H. kangerensis (MK569822)*	0.32	0.253	0.221	0.228	0.219	0.227	0.216	0.208	0.208	0.211	0.21																									
13	*H. kangerensis (MK569824)*	0.318	0.258	0.219	0.237	0.226	0.231	0.22	0.213	0.213	0.216	0.218	0.011																								
14	*H. kolliensis (MK569825)*	0.327	0.268	0.23	0.246	0.232	0.204	0.195	0.169	0.169	0.172	0.245	0.205	0.203																							
15	*H. kolliensis (MT943048)*	0.327	0.274	0.242	0.255	0.238	0.207	0.2	0.174	0.173	0.175	0.254	0.206	0.206	0.018																						
16	*H. maculatus (MK569827)*	0.304	0.265	0.208	0.242	0.229	0.224	0.207	0.211	0.211	0.209	0.221	0.175	0.172	0.216	0.214																					
17	*H. maculatus (MK569830)*	0.315	0.267	0.216	0.24	0.231	0.226	0.213	0.211	0.211	0.212	0.225	0.188	0.186	0.225	0.223	0.023																				
18	*H. paaragowli (MK802893)*	0.33	0.148	0.233	0.094	0.088	0.229	0.218	0.197	0.197	0.191	0.234	0.202	0.202	0.206	0.2	0.223	0.224																			
19	*H. paaragowli (MN496393)*	0.331	0.149	0.23	0.096	0.089	0.228	0.218	0.195	0.195	0.189	0.233	0.198	0.198	0.204	0.198	0.221	0.225	0																		
20	*H. pakkamalaiensis (OQ957153)*	0.348	0.269	0.251	0.245	0.231	0.213	0.207	0.087	0.088	0.104	0.237	0.221	0.227	0.184	0.188	0.22	0.225	0.194	0.192																	
21	*H. pakkamalaiensis (OQ957154)*	0.348	0.269	0.251	0.245	0.231	0.213	0.207	0.087	0.088	0.104	0.237	0.221	0.227	0.184	0.188	0.22	0.225	0.194	0.192	0																
22	*H. paucifasciatus (MK569847)*	0.33	0.287	0.231	0.273	0.249	0.238	0.225	0.225	0.225	0.222	0.229	0.177	0.18	0.215	0.217	0.174	0.177	0.239	0.236	0.231	0.231														
23	*H. paucifasciatus (OQ595083)*	0.324	0.309	0.235	0.278	0.247	0.241	0.226	0.223	0.223	0.222	0.239	0.172	0.174	0.216	0.219	0.169	0.175	0.238	0.234	0.231	0.231	0.003														
24	*H. prashadi (MK569843)*	0.326	0.261	0.227	0.248	0.229	0.23	0.214	0.21	0.21	0.211	0.226	0.193	0.194	0.218	0.217	0.191	0.198	0.224	0.224	0.218	0.218	0.211	0.212													
25	*H. sahgali (MG742362)*	0.316	0.263	0.23	0.256	0.242	0.238	0.234	0.231	0.231	0.232	0.237	0.195	0.194	0.223	0.229	0.178	0.182	0.21	0.206	0.237	0.237	0.162	0.163	0.228												
26	*H. scabriceps (MH454769)*	0.335	0.261	0.265	0.25	0.243	0.212	0.202	0.24	0.24	0.246	0.28	0.229	0.232	0.235	0.236	0.227	0.236	0.248	0.245	0.245	0.245	0.245	0.25	0.266	0.257											
27	*H. sirumalaiensis (MT943051)*	0.316	0.085	0.25	0.139	0.132	0.224	0.221	0.214	0.214	0.219	0.241	0.227	0.225	0.227	0.224	0.239	0.241	0.108	0.109	0.217	0.217	0.25	0.253	0.237	0.229	0.241										
28	*H. sirumalaiensis (MT943050)*	0.318	0.097	0.252	0.135	0.128	0.221	0.216	0.211	0.211	0.213	0.238	0.227	0.225	0.227	0.225	0.243	0.246	0.108	0.109	0.207	0.207	0.25	0.253	0.238	0.226	0.24	0.001									
29	*H. siva (MK569845)*	0.325	0.267	0.24	0.237	0.219	0.215	0.197	0.191	0.191	0.189	0.206	0.175	0.176	0.22	0.215	0.165	0.174	0.207	0.207	0.21	0.21	0.188	0.189	0.198	0.184	0.231	0.227	0.227								
30	*H. sushilduttai (MK569852)*	0.337	0.272	0.239	0.242	0.234	0.246	0.232	0.214	0.213	0.226	0.217	0.107	0.111	0.223	0.224	0.196	0.205	0.241	0.238	0.23	0.23	0.19	0.187	0.209	0.213	0.249	0.243	0.25	0.176							
31	*H. aaronbaueri (MN482222)*	0.299	0.275	0.106	0.266	0.258	0.232	0.221	0.217	0.216	0.228	0.274	0.206	0.209	0.208	0.215	0.218	0.222	0.233	0.23	0.236	0.236	0.239	0.247	0.21	0.235	0.252	0.258	0.254	0.221	0.228						
32	*H. triedrus (MH666065)*	0.309	0.284	0.236	0.257	0.245	0.236	0.224	0.238	0.238	0.232	0.254	0.198	0.196	0.209	0.22	0.182	0.187	0.23	0.227	0.239	0.239	0.164	0.168	0.214	0.172	0.248	0.235	0.233	0.169	0.213	0.221					
33	*H. vanam (MK569853)*	0.335	0.089	0.243	0.167	0.151	0.222	0.228	0.233	0.233	0.231	0.248	0.243	0.241	0.251	0.246	0.256	0.261	0.13	0.13	0.233	0.233	0.261	0.268	0.25	0.238	0.257	0.085	0.087	0.231	0.249	0.256	0.244				
34	*H. vanam (MK569854)*	0.332	0.098	0.244	0.164	0.151	0.232	0.236	0.231	0.231	0.231	0.262	0.236	0.233	0.246	0.242	0.244	0.248	0.129	0.129	0.238	0.238	0.26	0.266	0.246	0.242	0.251	0.084	0.085	0.231	0.242	0.257	0.248	0.001			
35	*H. vanam (MK569855)*	0.332	0.097	0.246	0.167	0.154	0.233	0.238	0.233	0.233	0.233	0.262	0.239	0.236	0.247	0.243	0.245	0.249	0.13	0.13	0.239	0.239	0.261	0.268	0.248	0.242	0.254	0.086	0.086	0.231	0.245	0.259	0.249	0	0.002		
36	*H. whitakeri (MH666066)*	0.325	0.256	0.248	0.245	0.236	0.217	0.209	0.217	0.216	0.223	0.238	0.195	0.197	0.226	0.228	0.172	0.177	0.208	0.205	0.227	0.227	0.163	0.169	0.234	0.118	0.246	0.229	0.229	0.166	0.215	0.245	0.17	0.248	0.248	0.249	

Table 3. Meristic and mensural data for the type series of *Hemidactylus multisulcatus* **sp. nov.,** *= broken tail, – = data not present, ? =broken finger. Measurements are in mm

Parameters	Holotype BNHS 2918	Paratype BNHS 2919	Paratype BNHS 2920
Sex	male	male	female
SVL	72.77	84.00	71.80
AG	30.28	37.44	27.49
TW	15.34	17.08	15.05
ED	4.87	5.23	4.90
EN	6.94	8.32	6.43
ES	8.20	10.48	8.07
ET	5.93	6.33	4.79
IN	2.52	2.88	2.26
EOD	2.11	2.24	1.80
HL	20.53	22.99	19.97
HW	14.36	16.80	13.60
HD	8.82	10.38	9.19
IO	7.49	8.12	7.17
UAL	12.95	15.95	13.82
FAL	13.83	14.91	12.61
PAL	8.43	8.78	8.29
FL1	3.24	3.56	2.61
FL2	4.52	4.11?	3.92
FL3	5.21	5.55	4.24
FL4	5.38	5.56	4.48
FL5	4.93	4.94	4.11
FEL	13.69	15.09	13.27
TBL	14.87	15.27	13.00
TOL1	3.24	3.64	2.40
TOL2	5.58	5.38	4.29
TOL3	5.33	6.07	4.70
TOL4	5.76	6.18	5.61
TOL5	5.36	5.97	5.13
TL	90.39*	89.96	88.72
SupL R/L	11/11	11/11	11/11
InfL R/L	9/10	9/10	9/10
SuS	30	30	28
InO	50	46	47
BeT	27	27	26
PoN	3	3	3
PoM	2	2	2
SuN	2	2	2
CaS	21	20	21
PvS	25	27	25
MbS	18	19	17
MvS	177	162	161
BlS	36	36	35
FPores	18/18	19/20	–
PS	7	6	–
MLam R	9/10/10/10/10	8/7?/11/11/11	8/10/10/10/10
PLam R	8/10/10/10/10	9/11/11/11/11	8/10/10/11/10

Carranza, S., Arnold, E. N., Mateo, J. A. and López-Jurado, L. F. 2000. Long-distance colonization and radiation in gekkonid lizards, Tarentola (Reptilia: Gekkonidae), revealed by mitochondrial DNA sequences. Proceedings of the Royal Society of London 267: 637–649.

Choung, C.M., Nickloff, B. J., Elias P. M., Goldsmith, L. A., Macher, E., Maderson, P. A., Sundberg, J. P., Tagami, H., Plongka, P. M., Thestrup-Pedersen, K., Bernard, B. A., Scroder, J. M., Dotto, P., Chang C, H., Williams, M. L., Feingold, K. R., King, L. E., Kligman, A. M., Rees, J. L. and Christophers, E. 2002. What is the 'true' function of skin. Exp. Dermatol 11: 159-187.

Das, S., Pal, S., Siddharth, S., Palot, M.J., Deepak, V. and Narayanan, S. 2022. A new species of large-bodied *Hemidactylus* Goldfuss, 1820 (Squamata: Gekkonidae) from the Western Ghats of India. Vertebrate Zoology 72: 81–94. https://doi.org/10.3897/vz.72.e76046

Edgar, R. C. 2004. MUSCLE: multiple sequence alignment with high accuracy and high throughput. Nucleic Acids Research 32 (5): 1792–1797.https://doi.org/10.1093/nar/gkh340

Gamble, T., Greenbaum, E., Jackman, T. R. and Bauer, A. M. 2012. Into the light: diurnality has evolved multiple times in geckos. Biological Journal of the Linnean Society 107(2): 328-348.

Giri, G. and Bauer, A. M. 2008. A new ground-dwelling *Hemidactylus* (Squamata: Gekkonidae) from Maharashtra, with a key to the *Hemidactylus* of India. Zootaxa 1700(1): 21-34.

Lanfear, R., Calcott, B., Ho, Y. W. S., and Guindon, S. 2012. PartitionFinder: Combined Selection of Partitioning Schemes and Substitution Models for Phylogenetic Analyses. Mol. Biol. Evol. 29 (6):1695–1701. doi:10.1093/molbev/mss020

Leary, S., Underwood, W. and Lilly, E., 2013. Guidelines for the Euthanasia of Animals. American Veterinary Medical Association.

Kalyaanamoorthy, S., Minh, B. Q. and Wong T. K. F. 2017. ModelFinder: Fast model selection for accurate phylogenetic estimates. Nature Methods 14: 587–589.

Khandekar, A., Thackeray, T. and Agarwal, I. 2021. A cryptic new species of rupicolous *Hemidactylus* Goldfuss, 1820 (Squamata: Gekkonidae) allied to *H. aaronbaueri* Giri, 2008 from the northern Western Ghats of Maharashtra, India. Zootaxa 5020 (3): 434–456.

Khandekar, A., Thackeray, T., Pawar, S. and Agarwal, I. 2020. A new medium-bodied rupicolous hemidactylus goldfuss, 1820 (Squamata: Gekkonidae) from the Sirumalai massif, Tamil Nadu, India. Zootaxa 4852: 83–100. https://doi.org/10.11646/zootaxa.4852.1.4

Kumar, S., Stecher, G., and Tamura, K. 2016. MEGA7: Molecular Evolutionary Genetics Analysis Version 7.0 for Bigger Datasets. Molecular biology and evolution 33: 1870– 1874.

Kluge, A. G. (1969) The evolution and geographical origin of the New World *Hemidactylus mabouia-brooki complex (Gekkonidae, Sauria). Miscellaneous Publications of the Museum of Zoology, University of Michigan 138: 1-78.*

Macey, J. R., Larson, A., Ananjeva and N.B. 1997. Two novel gene orders and the role of light-strand replication in rearrangement of the vertebrate mitochondrial genome. Molecular Biology and Evolution 14: 91–104.

Minh, B. Q., Schmidt, H. A,. Chernomor, O., Schrempf, D., Woodhams, M. D., Von Haeseler, A., Lanfear, R., and Teeling, E. 2020. IQ-TREE 2: New models and effi cient methods for phylogenetic inference in the genomic era. Molecular Biology and Evolution 37(5): 1530–1534. https://doi. org/10.1093/molbev/msaa015

Mohapatra, P. P., Agarwal, I., Mohalik, R. K., Dutta, S. K. and Khandekar, A. 2023. *Hemidactylus paucifasciatus* (Squamata: Gekkonidae), a new species of large-bodied, tuberculate gecko from Northern Odisha, India. Zootaxa 5301(3): 365–382.

Narayanan, S., Christopher, P., Raman, K., Mukherjee, N., Prabhu, P., Lenin, M., Vimalraj, S. and Deepak, V. 2023. A new species of rock-dwelling *Hemidactylus* Goldfuss, 1820 (Squamata: Gekkonidae) from the southern Eastern Ghats, India. Vertebrate Zoology 73, 2023: 499–512 DOI 10.3897/vz.73.e104494

Nguyen, L.T., Schmidt H. A., Von Haeseler A., and Minh B. Q. 2015. IQ-TREE: A fast and effective

stochastic algorithm for estimating maximum-likelihood phylogenies. Molecular Biology and Evolution 32: 268–274.

Pal, S. and Mirza, Z. A. 2022. A new species of Large-bodied Gecko of the genus *Hemidactylus* Goldfuss, 1820 from southern Western Ghats of Tamil Nadu, India. Journal of Bombay Natural History Society 119. https://doi.org/10.17087/jbnhs/2022/v119/167364

Rambaut, A., Drummond, A.J., Xie, D., Baele, G. and Suchard, M.A. 2018. Posterior summarization in Bayesian phylogenetics using Tracer 1.7. *S*ystematic Biology 67, 901–904. https://doi.org/10.1093/sysbio/syy032

Ronquist, F., Teslenko, M., Van Der Mark, P., Ayres, D.L., Darling, A., Höhna, S., Larget, B., Liu, L., Suchard, M.A. and Huelsenbeck, J.P. 2012. Mrbayes 3.2: Efficient bayesian phylogenetic inference and model choice across a large model space. Systematic Biology 61, 539–542. https://doi.org/10.1093/sysbio/sys029

Sayyed, A., Kirubakaran, S., Khot, R., Abinesh, A., Sayyed, A., Sayyed, M., Adhikari, O., Purkayastha, J., Deshpande, S. and Sulakhe, S. 2023. A New Rupicolous Day Gecko Species (Squamata : Gekkonidae : *Cnemaspis*) from Tamil Nadu , South India. 12, 5–13.

Scherz, M. D., Daza, J. D., Köhler, J., Vences, M. and Glaw, F. 2017. Off the scale: a new species of fish-scale gecko (Squamata: Gekkonidae: Geckolepis) with exceptionally large scales. PeerJ 5: e2955.

Schwarz, G. 1978. Estimating the Dimensions of a Model. The Annals of Statistics. Vol. 6, No, 2, 461–
464.

Tamura, K. and Nei, M. 1993. Estimation of the number of nucleotide substitutions in the control region of mitochondrial DNA in humans and chimpanzees. Molecular Biology and Evolution 10 (3): 512–526. https://doi.org/10.1093/oxfordjournals.molbev.a040023.

Uetz, P., Freed, P. and Hošek, J. 2022. The Reptile Database. Available from: http://www.reptile-database.org (accessed 7 July 2023)

Vanzolini, P. E. 1978. On South American Hemidactylus (Sauria, Gekkonidae). Papéis Avulsos de Zoologia 31(20): 307-343.

Vences, M. S., Wanke, D. R. V., Branch, W. R., Glaw, F. and Meyer, A. 2004. Natural colonization or introduction? Phylogeographical relationships and morphological differentiation of house geckos (Hemidactylus) from Madagascar. Biological Journal of the *Linnean Society* 83: 115-130.